Molecular Phylogenetics and Evolution 61 (2011) 79–89

Contents lists available at ScienceDirect

Molecular Phylogenetics and Evolution

journal homepage: www.elsevier.com/locate/ympev

# Molecular phylogenetic relationships and phenotypic diversity in miniaturized toadlets, genus *Brachycephalus* (Amphibia: Anura: Brachycephalidae)

Rute B.G. Clemente-Carvalho [a], Julia Klaczko [b], S. Ivan Perez [c], Ana C.R. Alves [d], Célio F.B. Haddad [d], Sérgio F. dos Reis [b,*]

[a] *Programa de Pós-Graduação em Genética, Universidade Estadual de Campinas, 13083-970 Campinas, São Paulo, Brazil*
[b] *Departamento de Biologia Animal, Universidade Estadual de Campinas, 13083-970 Campinas, São Paulo, Brazil*
[c] *División Antropología, Museo de La Plata, Universidad Nacional de La Plata, CONICET, Paseo del Bosque s/n, 1900 La Plata, Argentina*
[d] *Departamento de Zoologia, Universidade Estadual Paulista, 13506-900 Rio Claro, São Paulo, Brazil*

ARTICLE INFO

*Article history:*
Received 12 November 2010
Revised 2 May 2011
Accepted 27 May 2011
Available online 13 June 2011

*Keywords:*
Gene trees
Species tree
BEST
Amphibia
Geometric morphometrics
*Brachycephalus*
Brazil

ABSTRACT

Toadlets of the genus *Brachycephalus* are endemic to the Atlantic rainforests of southeastern and southern Brazil. The 14 species currently described have snout–vent lengths less than 18 mm and are thought to have evolved through miniaturization: an evolutionary process leading to an extremely small adult body size. Here, we present the first comprehensive phylogenetic analysis for *Brachycephalus*, using a multilocus approach based on two nuclear (*Rag-1* and *Tyr*) and three mitochondrial (Cyt *b*, 12S, and 16S rRNA) gene regions. Phylogenetic relationships were inferred using a partitioned Bayesian analysis of concatenated sequences and the hierarchical Bayesian method (BEST) that estimates species trees based on the multispecies coalescent model. Individual gene trees showed conflict and also varied in resolution. With the exception of the mitochondrial gene tree, no gene tree was completely resolved. The concatenated gene tree was completely resolved and is identical in topology and degree of statistical support to the individual mtDNA gene tree. On the other hand, the BEST species tree showed reduced significant node support relative to the concatenate tree and recovered a basal trichotomy, although some bipartitions were significantly supported at the tips of the species tree. Comparison of the log likelihoods for the concatenated and BEST trees suggests that the method implemented in BEST explains the multilocus data for *Brachycephalus* better than the Bayesian analysis of concatenated data. Landmark-based geometric morphometrics revealed marked variation in cranial shape between the species of *Brachycephalus*. In addition, a statistically significant association was demonstrated between variation in cranial shape and genetic distances estimated from the mtDNA and nuclear loci. Notably, *B. ephippium* and *B. garbeana* that are predicted to be sister-species in the individual and concatenated gene trees and the BEST species tree share an evolutionary novelty, the hyperossified dorsal plate.



## 1. Introduction

The New World frogs recently classified as the Terrarana comprise five monophyletic clades which are formally recognized as the families Brachycephalidae, Ceuthomantidae, Craugastoridae, Eleutherodactylidae, and Strabomantidae (Hedges et al., 2008; Heinicke et al., 2009). The species of Terrarana share an advanced reproductive mode characterized by terrestrial breeding and direct development of terrestrial eggs that bypass the tadpole stage and hatch into froglets (Lynch and Duellman, 1997). Direct development and the production of small, isolated clutches are life-history traits that contribute to promoting population structuring (Dubois, 2004) and are likely to explain the high diversity of the Terrarana, which currently comprise ~1000 species (Hedges et al., 2008; Heinicke et al., 2009).

Due to their wide geographical distribution, broad elevation range, and species diversity, the Terrarana are a prime model group for addressing questions in ecology, biogeography, and conservation in the Neotropics. This task fundamentally requires knowledge and understanding of evolutionary relationships and, for the family Brachycephalidae within the Terrarana, this information is sorely lacking (Heinicke et al., 2007). The Brachycephalidae is a monophyletic clade distributed in the Atlantic Forest in eastern Brazil and in the *Araucaria* forest in southeastern and southern Brazil and northern Argentina, and includes the genera *Brachycephalus* and *Ischnocnema* (Hedges et al., 2008). The genus *Brachycephalus*, which is the focus of this report, is endemic to the Atlantic rainforests of southeastern and southern Brazil, and 14 species are currently recognized (Haddad et al., 2010). Amongst these 14 species, *B. ephippium garbeana* which was usually considered to

* Corresponding author. Fax: +55 19 3521 6358.
*E-mail address:* sfreis@unicamp.br (S.F. dos Reis).

1055-7903/$ - see front matter © 2011 Elsevier Inc. All rights reserved.
doi:10.1016/j.ympev.2011.05.017

be a synonym of *B. ephippium* (Cochran, 1955), has been recently granted full species status (*B. garbeana*; Pombal, 2010). The species of *Brachycephalus* are well characterized and diagnosed on the basis of skin color, osteological traits, and morphometric features, although in most cases they are known only from their type localities (Alves et al., 2006, 2009; Pombal and Gasparini, 2006; Haddad et al., 2010; Pombal, 2010). All species of *Brachycephalus*, except for *B. didactylus* and *B. hermogenesi*, occur in isolation in mountain ranges at elevations ranging from 600–1800 m (Pombal et al., 1998; Pombal, 2001; Ribeiro et al., 2005; Alves et al., 2006). The latter two species, which were formerly placed in *Psyllophryne* (Izecksohn, 1971; Giaretta and Sawaya, 1998), occur at sea level and from sea level up to 900 m (Pimenta et al., 2007; Verdade et al., 2008), respectively.

*Brachycephalus* species exhibit striking variation in color (Fig. 1), and in some species, an aposematic coloration is associated with tetrodotoxin toxicity (Pires et al., 2002, 2005; Hanifin, 2010). *Brachycephalus* species are also a remarkable example of miniaturization, which is an evolutionary process leading to extremely small adult body size (Trueb and Alberch, 1985; Hanken, 1993; Hanken and Wake, 1993; Yeh, 2002). All species of *Brachycephalus* have a snout–vent length <1.8 cm and share morphological features that are typically associated with miniaturization, including the loss of some bones and a reduced number of fingers and toes (Alves et al., 2006; Pombal and Gasparini, 2006). Another outstanding phenotypic feature among the species of *Brachycephalus* is a gradient in the degree of mineralization of the skeleton, ranging from a hyperossified condition of the skull and vertebrae to a complete lack of hyperossification (Clemente-Carvalho et al., 2009).

The observed phenotypic diversity and the montane distribution of most of these species, which creates natural allopatry among component populations and species, makes *Brachycephalus* a potentially promising reference system to explore geographic models of speciation and biogeographic processes. However, we currently lack a hypothesis for the phylogenetic relationships of *Brachycephalus*. Furthermore, important aspects of phenotypic diversity, including shape variation in complex morphological structures such as the skull, have not yet been assessed for *Brachycephalus*. As such, this study was designed to answer the following questions. (1) What are the phylogenetic relationships among species of *Brachycephalus*? Here this question is addressed by two approaches: a partitioned Bayesian analysis of concatenated sequences (Ronquist and Huelsenbeck, 2003) and the coalescent framework that simultaneously estimate gene trees and species trees from multilocus data (Edwards et al., 2007; Liu and Pearl, 2007; Knowles and Kubatko, 2010; Castillo-Ramirez et al., 2010). (2) Is there a statistical association between phenotypic patterns of variation in cranial shape and molecular phylogenetic relationships?

## 2. Materials and methods

### 2.1. Biological samples

Tissue samples from muscle or liver were taken from voucher specimens of all currently known species of *Brachycephalus* (Table 1). Molecular data and analyses have established *Ischnocnema* as the sister group of *Brachycephalus* (Hedges et al., 2008), and *I. parva* is used here as outgroup. Five genes were targeted for amplification and sequencing: three mitochondrial genes, Cyt *b*, 12S rRNA, and 16S rRNA, and two nuclear genes, *Rag-1* and *Tyr*. We sequenced one specimen per taxon per gene, with the exception of *B. hermogenesi* for the 16S rRNA gene. The complete list of voucher numbers and associated localities are given in Table 1 and Fig. 2.

### 2.2. DNA isolation, amplification and sequencing

Genomic DNA was extracted from liver (or muscle) tissue preserved in 100% ethanol. Tissue samples were digested with proteinase K, and we then followed a standard three-step phenol/chloroform extraction procedure (Sambrook et al., 1989). The sequences used in this study were obtained for three mitochondrial and two nuclear genes. Fragments of the mitochondrial cytochrome *b* (Cyt *b*) and 12S rRNA genes were amplified using the primers and parameters given in Goebel et al. (1999). A segment of the mitochondrial 16S rRNA gene was amplified using the primers and specifications given in Darst and Cannatella (2004). Fragments of the nuclear genes *Rag-1* and *Tyr* were amplified using the primers and parameters given in Hedges et al. (2008). The amplification products were visualized on 1.0% agarose gels and purified using a GFXTM PCR DNA and Gel Band Purification kit (GE Healthcare). Purified PCR products were outsourced to Macrogen Inc. in Seoul, South Korea, for sequencing (using the BigDyeTM terminator kit and run on an ABI 3730XL). Sequences were obtained in both directions with the same primers used for PCR amplification and subjected to BLAST searches (Altschul et al., 1997) in GenBank to verify that the desired sequences had been amplified. Sequence traces were analyzed using the *phred* program (Ewing et al., 1998). We obtained a total of 4563 base pairs of which 964 were from the Cyt *b;* 965 from 12S; 1416 from 16S; 656 from *Rag-1*; and 562 from *Tyr*. The authenticity of the genes was confirmed by amino acid translation. All sequences were

**Fig. 1.** Photographs of some species of *Brachycephalus*; from left to right (top and bottom): *Brachycephalus brunneus*, *B. ferruginus*, *B. hermogenesi*, *B. garbeana*, *B. pitanga*, and *B. toby*.

**Table 1**
Species, voucher, sampling localities, elevation, and geographic coordinates of the specimens for which mitochondrial and nuclear markers were sequenced in the current study.

| Species | Voucher | Location (ID No. on Fig. 2) | Elevation (m) | Coordinates |
|---|---|---|---|---|
| *Brachycephalus alipioi* | CFBH 3566 | Vargem Alta, Espírito Santo (1) | 1100 | 20°28′S–41°00′W |
| *Brachycephalus garbeana* | CFBH 16800 | Macaé de Cima, Rio de Janeiro (2) | 1130 | 22°28′S–42°12′W |
| *Brachycephalus didactylus* | CFBH 12907 | Ilha Grande, Rio de Janeiro (3) | 0 | 23°05′S–44°16′W |
| *Brachycephalus vertebralis* | CFBH 7907 | Ubatuba, São Paulo (4) | 813 | 23°09′S–44°45′W |
| *Brachycephalus hermogenesi* | CFBH 12908 | Piedade, São Paulo (5) | 780 | 23°42′S–47°25′W |
| *Brachycephalus pitanga* | CFBH 16746 | São Luís do Paraitinga, São Paulo (6) | 920 | 23°20′S–45°08′W |
| *Brachycephalus toby* | CFBH 23002 | Ubatuba, São Paulo (7) | 750 | 23°27′S–45°11′W |
| *Brachycephalus ephippium* | CFBH 16807 | Atibaia, São Paulo (8) | 850 | 23°07′S–46°33′W |
| *Brachycephalus nodoterga* | CFBH 6211 | Serra da Cantareira, São Paulo (9) | 750 | 23°42′S–46°65′W |
| *Brachycephalus brunneus* | CFBH 7905 | Campina Grande do Sul, Paraná (10) | 1300 | 25°23′S–48°83′W |
| *Brachycephalus pernix* | CFBH 2597 | Quatro Barras, Paraná (11) | 1400 | 25°38′S–49°08′W |
| *Brachycephalus ferruginus* | CFBH 8025 | Morretes, Paraná (12) | 1200 | 25°43′S–48°92′W |
| *Brachycephalus pombali* | CFBH 8043 | Guaratuba, Paraná (13) | 1300 | 25°65′S–48°85′W |
| *Brachycephalus izecksohni* | CFBH 7374 | Paranaguá, Paraná (14) | 1000 | 25°78′S–49°38′W |

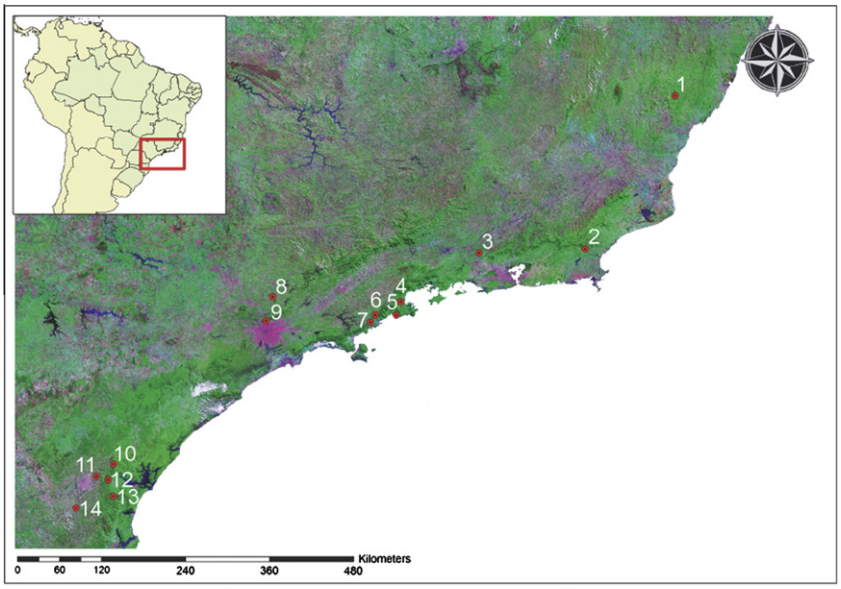


**Fig. 2.** Map of southeastern and southern Brazil showing the geographic locations of the sampling sites of *Brachycephalus* (1–14 which correspond to site ID used in Table 1).

deposited in GenBank with the following accession numbers: Cyt *b* (HQ435703–HQ435717), 12S rRNA (HQ435676–HQ435689), 16S rRNA (HQ435690–HQ435702), *Rag-1* (HQ435718–HQ435731), and *Tyr* (HQ435732– HQ435745).

### 2.3. Molecular data analysis

Sequences were aligned using ClustalX 2.0 (Larkin et al., 2007). The alignments are available at TreeBase (Piel et al., 2009) with submission number 11473. Each locus was evaluated to identify the most appropriate evolutionary model using JModeltest 0.1.1 (Posada, 2008) and selected the model favored under the Bayesian information criterion (BIC).

The gene trees were estimated for individual nuclear locus partitions and for the combined mitochondrial dataset, using Bayesian inference, implemented in Mr. Bayes v3.1.2 (Huelsenbeck and Ronquist, 2001; Ronquist and Huelsenbeck, 2003). The analyses consisted of two runs, with default heating for each of the four chains and sampling every 1000 generations for 1,000,000 generations. The convergence was verified using the program Tracer v1.4 (Rambaut and Drummond, 2007); and the first 500 topologies (5% of the sampled topologies) were discarded as burn-in.

The concatenated analysis was done using both nuclear loci plus mitochondrial dataset as a partition, and assigned its own substitution model. As in the individual gene analyses, we performed two runs, with default heating for each of the four chains and sampling every 1000 generations for 1,000,000 generations. The convergence was verified using the program Tracer v1.4 (Rambaut and Drummond, 2007); and the first 500 topologies (5% of the sampled topologies) were discarded as burn-in.

The species tree was obtained using the Bayesian hierarchical model (Liu and Pearl, 2007) to estimate a distribution of species trees from vectors of estimated gene trees, across multiple loci, using the software BEST (Liu, 2008). We excluded the gene 16S from the analysis, because the *B. hermogenesi* sequence was not available for this gene, as recommend in the BEST manual. Individual taxa missing for an entire locus can be misleading, since the placement of the taxa will be purely derived from the priori distribution. All the Bayesian model specifications in BEST followed the MrBayes settings. The priori distribution of the scaled population size ($\theta$) was an inverse gamma distribution and we used the default settings alpha (3.0) and beta (0.03) (Liu and Pearl, 2007). Two runs with two Markov chains each were conducted through 100 million generations, with trees being sampled every 1000 generations and a conservative burn-in at 500,000.

### 2.4. Phenotypic data analysis

The specimens examined in our phenotypic analyses of variation are deposited in the following public herpetological collec-

tions: (1) the Adolpho Lutz collection, deposited in the Museu Nacional, Rio de Janeiro, Rio de Janeiro, Brazil; and (2) the Célio F. B. Haddad collection, deposited in the Departamento de Zoologia, Universidade Estadual Paulista, Campus de Rio Claro, São Paulo, Brazil. The sample sizes used in the morphometric analyses were as follows: *B. alipioi*, Vargem Alta, State of Espírito Santo ($n = 10$); *B. brunneus*, Campina Grande do Sul, State of Paraná ($n = 15$); *B. didactylus*, Paulo de Frontin, State of Rio de Janeiro ($n = 17$); *B. ephippium*, Atibaia, State of São Paulo ($n = 20$); *B. ferruginus*, Morretes, State of Paraná ($n = 17$); *B. garbeana*, Macaé de Cima, State of Rio de Janeiro ($n = 19$); *B. hermogenesi*, Ubatuba, State of São Paulo ($n = 3$); *B. izecksohni*, Paranaguá, State of Paraná ($n = 10$); *B. nodoterga*, Serra da Cantareira, State of São Paulo ($n = 16$); *B. pernix*, Quatro Barras, state of Paraná ($n = 27$); *B. pitanga*, São Luís do Paraitinga, state of São Paulo ($n = 16$); *B. pombali*, Guaratuba, State of Paraná ($n = 8$); *B. toby*, Ubatuba, State of São Paulo ($n = 13$); and *B. vertebralis*, Parati, State of Rio de Janeiro ($n = 13$). Because the majority of species of *Brachycephalus* are known only from the type locality, one population sample per species was analyzed with the statistical procedures described below.

The variation in cranial shape among the species of *Brachycephalus* was assessed on the basis of 15 anatomical (cranial) landmarks. These landmarks were chosen to sample relevant features of cranial morphology as previously described by Clemente-Carvalho et al. (2008). They are defined as follows (Fig. 3): (1) anterior end of suture between premaxillae; (2) tip of the palatine process on the premaxilla; (3) anteriormost corner of the frontoparietal; (4) anterior end of suture between frontoparietals; (5) anterolateral corner of the frontoparietal; (6) anterior end of the projection of the pars facialis; (7) maximum anterior curvature of the otic capsule; (8) anterior end of the projection of the parotic plate overlying the prootic; (9) tip of the zygomatic ramus on the squamosal; (10) latero-posterior end of the prootic; (11) medial-posterior end of the prootic; (12) posterior curvature of the prootic; (13) anterolateral curvature of prootic; (14) anterior tip of the occipital condyle; and (15) center of the foramen magnum. The *x*- and *y*-coordinates of each landmark were obtained using tpsDig software (Rohlf, 2006) on microradiographs taken with an X-ray microfocus tube and an image plate detector (Rocha et al., 2007). Because of symmetry, landmarks were defined from only one side of the skull. The use of landmarks from a single side of a symmetric structure is widely accepted (Larson, 2004; Fabrezi, 2006), as long as the interest of the study is not focused on asymmetric components. Furthermore, the use of redundant landmarks artificially inflates the number of dimensions in shape space, requiring larger sample sizes for statistical analyses and generating rank deficient matrices, which demand special techniques for analysis (Klingenberg et al., 2002). The differences in location, scaling, and orientation of landmarks were removed using a generalized Procrustes analysis (Rohlf and Slice, 1990; Bookstein, 1991). Following the Procrustes analysis, the aligned landmarks were subjected to relative warps analysis (i.e., a principal components analysis; Bookstein, 1991; Rohlf, 1993), to determine the principal directions of variation in cranial shape among the population samples of *Brachycephalus*. Differences in cranial shape among the species of *Brachycephalus* were visualized as deformation grids (Rohlf 1993; Adams et al., 2004). In these statistical analyses males and females were combined due to the lack of significant sexual dimorphism in cranial shape (Clemente-Carvalho et al., 2008, 2009).

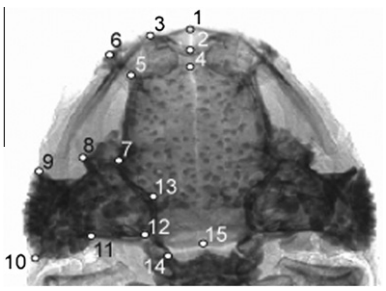


**Fig. 3.** Morphological landmarks depicted as circles on a dorsal view of an X-ray microradiograph of the skull of *Brachycephalus ephippium*. See text for the definition of numbered landmarks.

The skeletons of two specimens (one male and one female) were prepared for scanning electron microscopy. These specimens were selected as representatives of the gradient in the degree of mineralization and ossification among the species of *Brachycephalus*, as determined by the examination of X-ray microradiographs from all samples (see Clemente-Carvalho et al., 2009 for details of X-ray microradiograph methodology). The specimens were immersed in a solution of sodium hypochlorite for removal of the soft tissues and then air dried as described in Clemente-Carvalho et al. (2009). The skeletons were then mounted onto metal stubs, coated with gold in a Sputter Coater Balzers SCD050 machine, and examined under a Jeol JSM 5800LV scanning electron microscope.

The matrices based on Euclidean shape distance (i.e., the shape distance in the tangent space) and observed (uncorrected) molecular distance among all *Brachycephalus* species were compared using the PROTEST method (Gower, 1971; Peres-Neto and Jackson, 2001). First, the Euclidean shape and the molecular distance matrices were represented as a set of coordinate axes using principal coordinates (when performed on Euclidean distances, this analysis generates the same results as the relative warps analysis based on landmark data) and multidimensional scaling ordination analyses, respectively. Then, we scale and rotate these ordinations, using a minimum squared differences criterion, in order to find an optimal superimposition that maximizes their fit. The sum of the squared residuals between configurations in their optimal superimposition can then be used as a measurement of association ($m_{12}$; Gower, 1971). Finally, a permutation procedure (10,000 permutations) was used to assess the statistical significance of the optimal superimposition (Peres-Neto and Jackson, 2001). The PROTEST analysis was made using vegan 1.17–0 package for R 2.10.1 (R Development Core Team, 2010).

## 3. Results

### 3.1. Molecular data analysis

The uncorrected sequence divergence across ingroup taxa was variable among loci of nuclear and mitochondrial genes. The nuclear genes *Rag-1* and *Tyr* show a range of 0–0.06 and 0–0.08, respectively, whereas the mitochondrial loci show a higher variation between their loci, ranging from 0.007 to 0.23. Individual gene tree topologies are marked at nodes significantly supported (Fig. 4; $\geqslant$95% posterior probability, Huelsenbeck and Rannala, 2004). The mitochondrial gene tree is completely resolved (Fig. 4A). On the other hand, the nuclear gene trees show reduced levels of node support with the unresolved relationships appearing primarily at the tips of trees (Fig. 4B and C).

The concatenated tree topology was fully resolved and all bipartitions were significantly supported ($\geqslant$95% posterior probabilities; Fig. 5). Two major clades were revealed: the first has *B. brunneus* and *B. izecksohni* as sister to *B. pombali*, *B. ferruginus*, and *B. pernix*. The second clade shows a nested structure in which *B. didactylus* is basal to a clade in which *B. ephippium* and *B. garbeana* have a sister relationship with a group of species including *B. alipioi* and *B. hermogenesi* as sister to *B. pitanga* and *B. vertebralis* and *B. nodoterga* and *B. toby*.

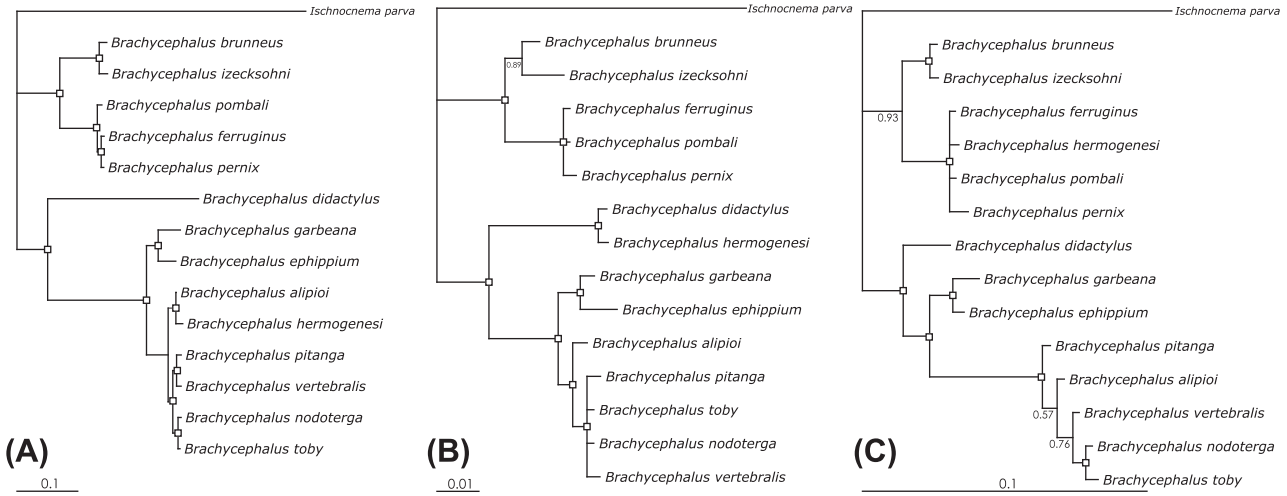


**Fig. 4.** Individual gene tree estimates. Nodes with greater than 95% posterior probability support are marked with a box (□); Branch lengths are in substitutions/site. A. Mitochondrial loci. B. *Rag*-1 nuclear gene. C. *Tyr* nuclear gene.

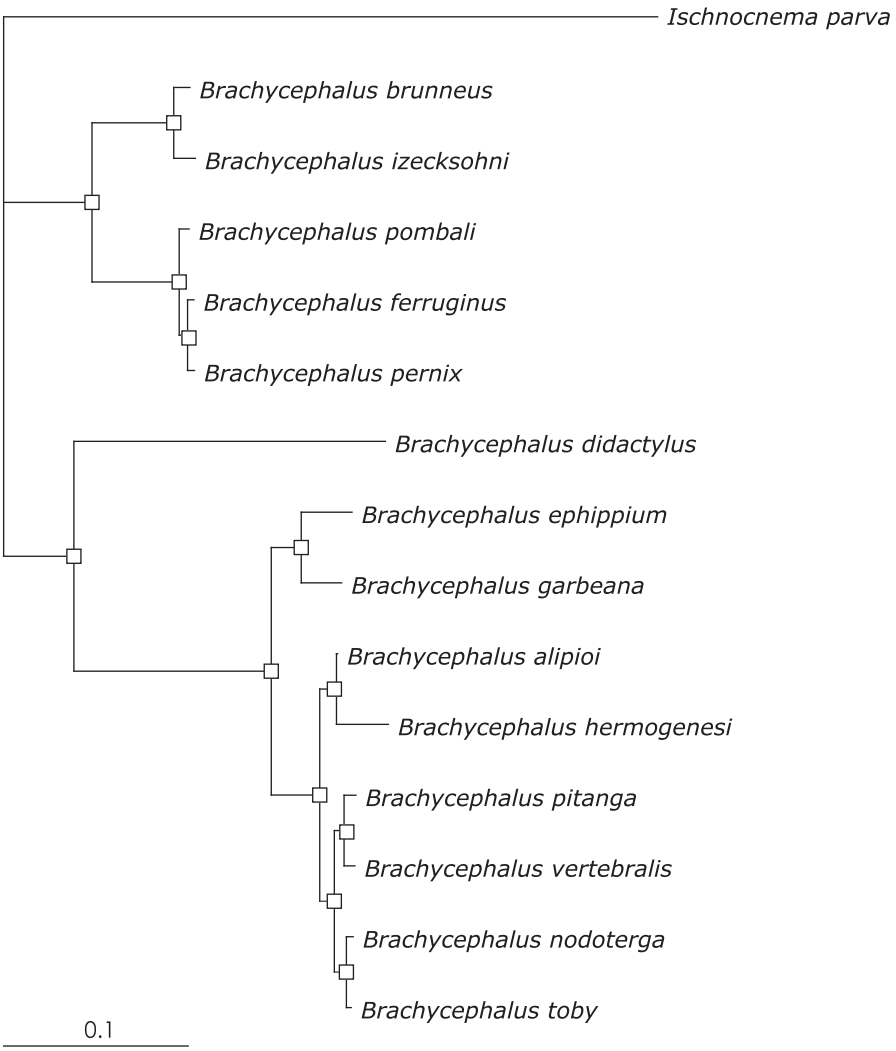


**Fig. 5.** Concatenated tree from the partitioned Bayesian analysis for the mitochondrial and nuclear genes. Nodes with greater than 95% posterior probability support are marked with a box (□); branch lengths are in substitutions/site.

Comparison between the individual gene trees reveals both support and conflict with respect to the concatenated tree. The concatenated tree is identical to the individual mtDNA gene tree both in topology and degree of statistical support (Figs. 4A and 5). On the other hand, the concatenated tree differs from the two nuclear gene trees in the reduced node support of the latter and

also in topology (Figs. 4B, C and 5). The differences in topology appear to be caused primarily by a single taxon, *B. hermogenesi*, which shares distinct phylogenetic liaisons in each of the nuclear gene trees and the concatenated tree. For the sake of comparison, we also computed the concatenated tree for the two nuclear genes (Fig. 6). The level of node support for the concatenated nuclear gene tree is slightly higher than for each individual nuclear gene tree (Figs. 4B, C and 6). Again, the topological discordances between the concatenated nuclear gene tree and the individual nuclear gene trees appear to be caused by the positioning of *B. hermogenesi*.

The species tree obtained from the BEST analysis recovered a basal trichotomy between a lineage leading to *B. ephippium* and *B. garbeana*, a lineage containing *B. brunneus*, *B. izecksohni*, *B. pombali*, *B. ferruginus*, and *B. pernix*, and another lineage which includes *B. didactylus*, *B. hermogenesi*, *B. alipioi*, *B. pitanga*, *B. vertebralis*, *B. nodoterga*, and *B. toby* (Fig. 7). To compare the BEST method with the concatenation method we plotted the log likelihoods for all post-burn-in trees (Fig. 8). The log likelihoods for trees from each method are tightly grouped and well separated, with the likelihood derived from the BEST method being much greater than that of the concatenation method. This result suggests that the method implemented in BEST explain the multilocus data for *Brachycephalus* better than the Bayesian analysis of concatenated data.

### 3.2. Phenotypic data analysis

The first two relative warps explain 78.5% of the total variation in skull shape among the species of *Brachycephalus* (Fig. 9A). The cranial shape for each species is represented by its mean values, which are depicted as black dots on the reduced space of the first and second relative warps. Overall, three clusters based on similarity of cranial shape can be discerned. One cluster includes *B. ephippium* from the state of São Paulo and *B. garbeana*, which occurs in the state of Rio de Janeiro in Southeastern Brazil (Fig. 9A). Electron scanning microscopy revealed that in *B. ephippium* and *B. garbeana*, hyperossification manifests itself as a bony growth projecting outward from the surface of the skull (exostosis; Fig. 9A). In *B. ephippium* and *B. garbeana*, the development of a hyperossified dorsal shield lying above the presacral vertebrae and transverse processes is also observed. A second cluster includes *B. alipioi*, *B. toby*, *B. nodoterga*, *B. pitanga*, and *B. vertebralis*, which also occur in southeastern Brazil (Fig. 9A). These species also exhibit a hyperossified skull, but the degree of hyperossification is not as developed as in *B. ephippium* and *B. garbeana*. Furthermore, these species do not have a bony dorsal shield (Fig. 9A). Hyperossification of the post-cranial skeleton is restricted to the distal end of the process of the fourth vertebra and spinal process of vertebrae (Fig. 9A). The third cluster joins *B. brunneus*, *B. didactylus*, *B. ferruginus*, *B. hermogenesi*, *B. ize-*

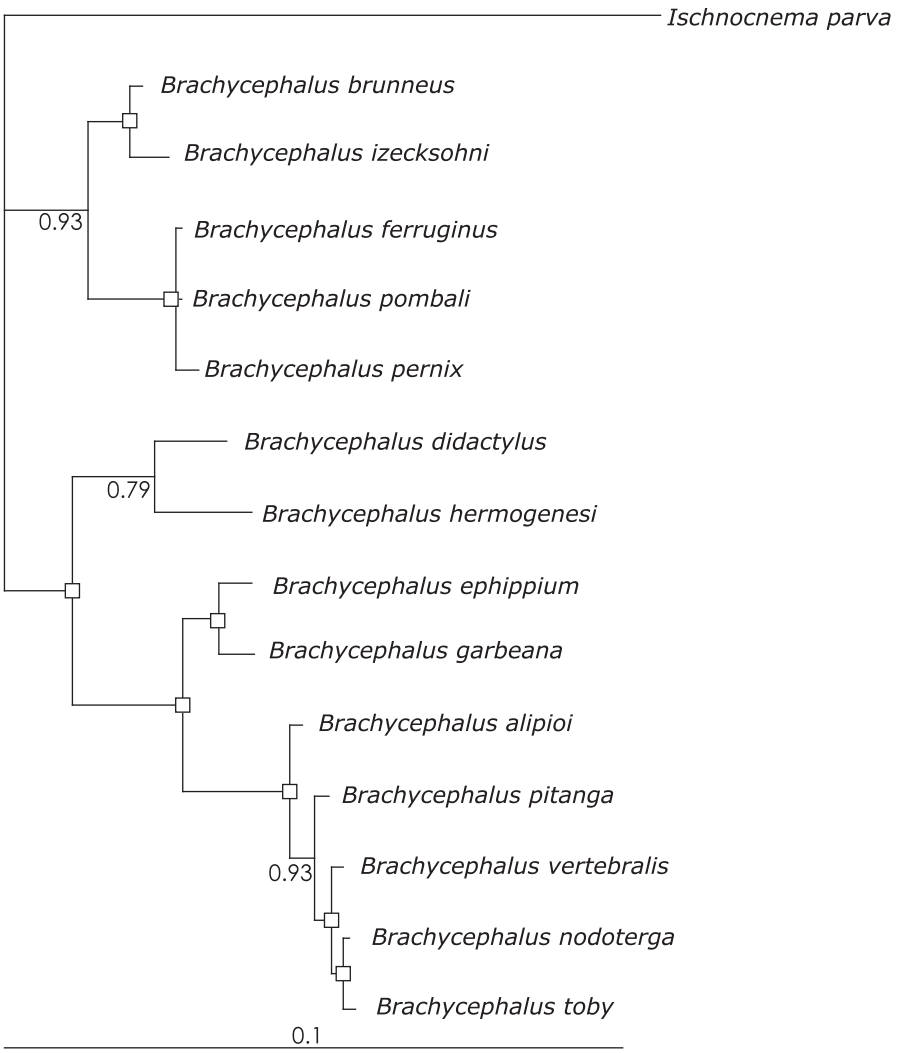


**Fig. 6.** Concatenated tree from the partitioned Bayesian analysis for the nuclear genes. Nodes with greater than 95% posterior probability support are marked with a box (□); branch lengths are in substitutions/site.

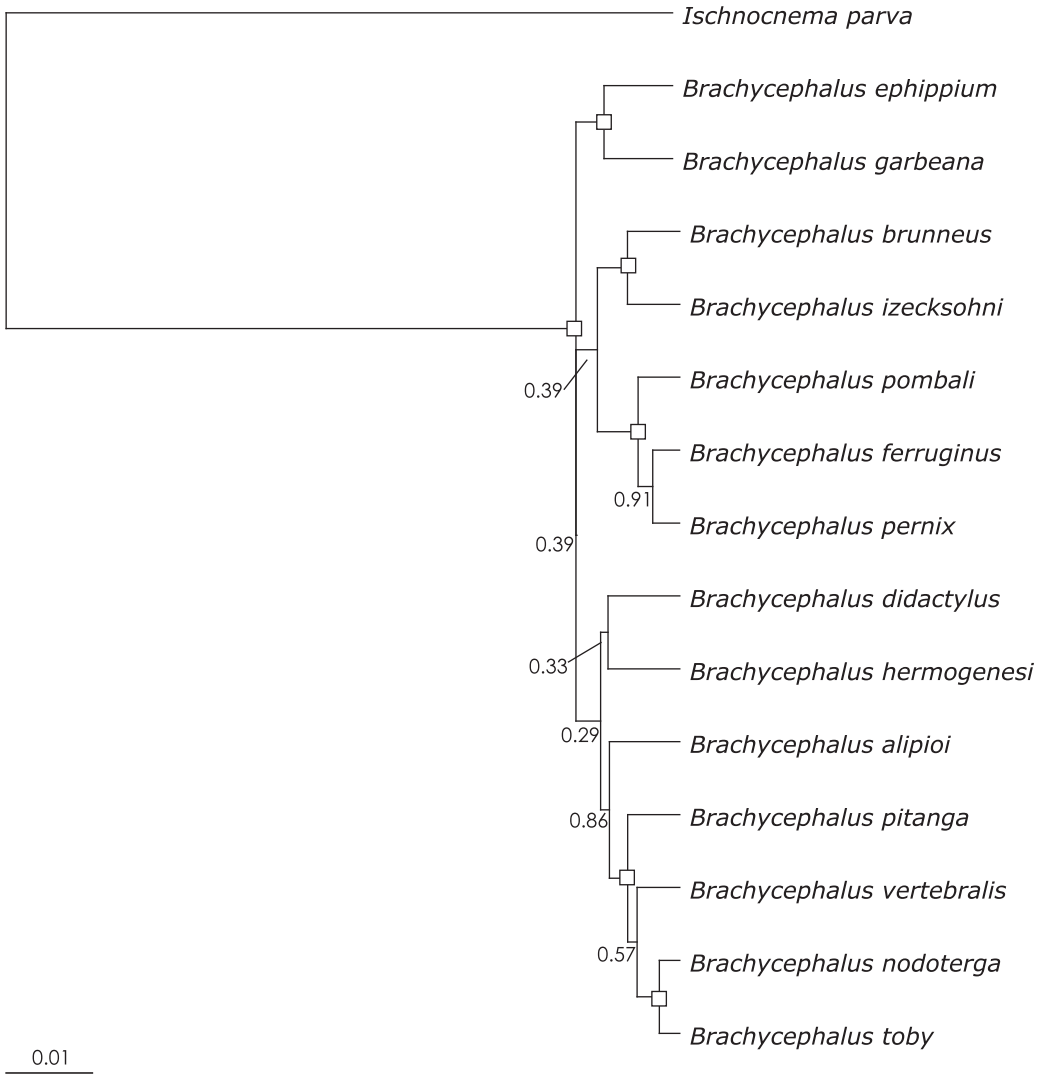


**Fig. 7.** BEST species tree. Nodes with greater than 95% posterior probability support are marked with a box (□); branch lengths are in substitutions/site.

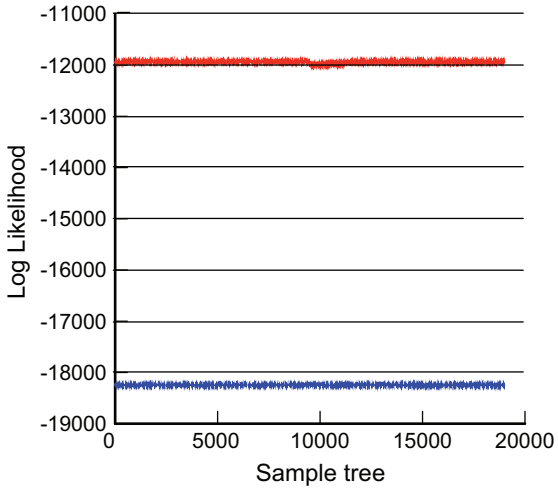


**Fig. 8.** Plot of the log likelihoods for posterior trees (after removal of burn-in trees). The curve on the top is for the likelihood of the hierarchical BEST model and the second is the likelihood for the concatenated Bayesian partitioned analysis.

*cksohni*, *B. pernix*, and *B. pombali*, in which the skull and vertebrae are completely devoid of hyperossification (Fig. 9A). All species in this cluster, with the exception of *B. didactylus* and *B. hermogenesi*, are restricted in distribution to southern Brazil. Changes in cranial shape implied by the first relative warp show mainly changes in the parotic plate, with *B. ephippium* and *B. garbeana* characterized by widest and largest parotic plate (Fig. 9B and C). Conversely, deformations depicted by the second relative warp display changes in the nasal cavity, with *B. pitanga* and *B. toby* having the widest nasal cavity (Fig. 9D and E).

The visual comparison of variation in cranial shape described by the RWs and the molecular distances between the species of *Brachycephalus* shows a high correspondence (Fig. 10). The PROTEST analysis confirms this visual interpretation, showing a high degree of association between the Procrustes distances and the molecular distances calculated with nuclear genes ($m_{12} = 0.832$; $P = 0.0001$), mitochondrial sequences ($m_{12} = 0.693$; $P = 0.0029$), and the combined dataset ($m_{12} = 0.746$; $P = 0.0005$).

## 4. Discussion

### 4.1. Gene trees versus concatenated tree versus species tree

A noteworthy aspect of our results is that the mtDNA gene tree is completely resolved with all nodes statistically supported by

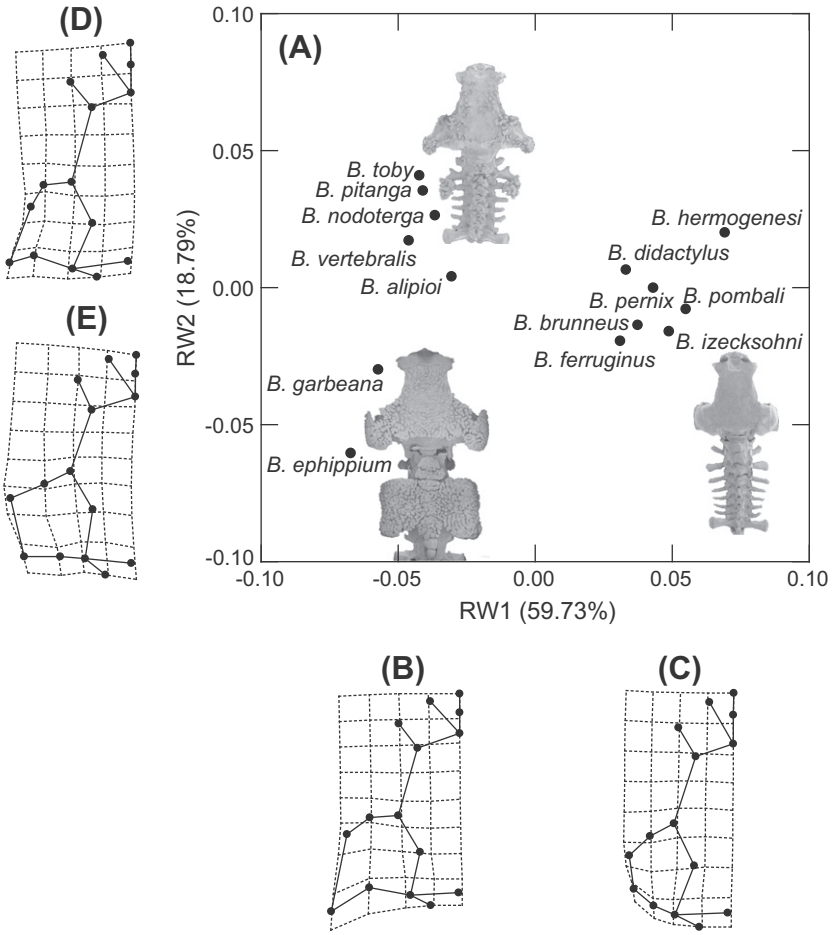


**Fig. 9.** (A) Ordination of species of *Brachycephalus* in the space of the first and second relative warps (RW). The percentage of variation explained by RW1 and RW2 are given in parenthesis. Each dot represents the mean cranial shape of a species. (B–E) Estimated changes in cranial shape are shown as deformations implied by the first and second relative warps for positive and negative deviations from the mean. Electron scanning microscopy images of skeletons are shown beside each major cluster of species based on cranial shape.

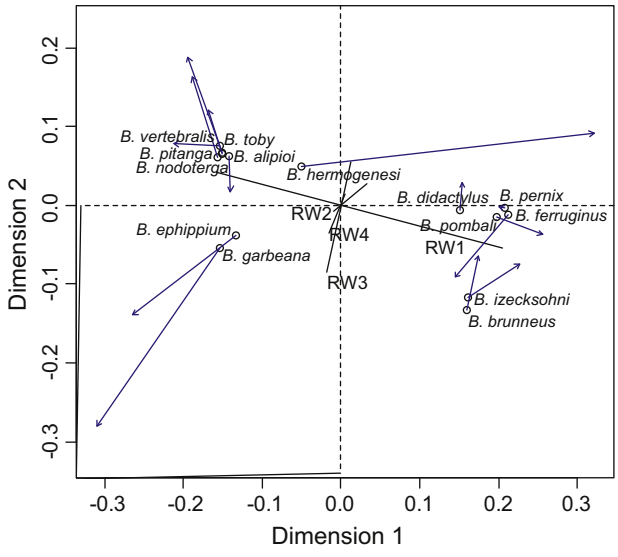


**Fig. 10.** PROTEST superimposition of *Brachycephalus* species ordination based on the four dimensions of the multidimensional scaling analysis for the molecular distances (circles; this ordination was defined as the reference in the graph) and the four first relative warps (end point of solid lines). Solid lines represent Procrustes residuals from both ordinations.

posterior probabilities ⩾95%, whereas each individual nuclear gene tree is less resolved than the mtDNA gene tree. The fully resolved branching order in the mtDNA gene tree, as compared to the nuclear gene trees, may be attributed to the fact that the mitochondrial genes should sort to monophyly four times faster than any single nuclear locus (Ballard and Whitlock, 2004; Zinc and Barrowclough, 2008; Brito and Edwards, 2009). Close inspection of gene trees revealed some strongly supported (posterior probabilities ⩾95%) relationships between species of *Brachycephalus* that are consistent among individual gene trees. In fact, the topological discordances between the gene trees appear to be caused primarily by a single taxon, *B. hermogenesi*, which shares distinct phylogenetic liaisons in each of the gene trees.

Our partitioned Bayesian analysis generated a concatenated tree for *Brachycephalus* that is identical in topology and degree of statistical support (posterior probabilities ⩾95%) to the individual mtDNA gene tree. An inherent factor in the concatenation approach is that a high confidence in the concatenated tree can be the outcome of one or a few gene loci that contribute a greater fraction of nucleotides (and possibly variable sites) to the multilocus data set (Mossel and Vigoda, 2005; Pasachnik et al., 2010; Brito and Edwards, 2009). Here, the results show that the concatenated tree is being overridden by the mtDNA loci due to its disproportionate contribution to the data partition relative to the nuclear genes, as has been demonstrated in other studies (e.g., Pasachnik

et al., 2010). It worthy mentioning in this connection that the concatenated nuclear gene tree also displays a high degree of support for most of the nodes—a remarkable result given that the number of informative sites in any individual nuclear coding sequence is typically small leading to poor phylogenetic resolution (Brito and Edwards, 2009). The concatenated nuclear gene tree and the concatenated gene tree for all data partitions predict the same phylogenetic relationships for some taxa of *Brachycephalus*, but the topological discordances remain as a function of the changing position of *B. hermogenesi*.

The concatenation approach is based on the assumption that all sequences evolved according to a single evolutionary tree, although it allows for different mutation rates and models of substitution for different sites (Degnan and Rosenberg, 2009). However, it is now well established from a theoretical standpoint that individual gene trees may differ in topology from each other and from the species tree due to the stochastic nature of lineage sorting during speciation (Degnan and Rosenberg, 2009). Therefore, the multispecies coalescent approach which estimates the species tree directly from a multilocus DNA sequence data (Edwards et al., 2007; Liu and Pearl, 2007; Degnan and Rosenberg, 2009; Liu et al., 2009) has been shown instrumental in revealing the evolutionary history of groups of closely related species. The main contrast between the concatenated tree and BEST species tree observed here for the multilocus data set of *Brachycephalus* is the reduced level of support in the latter. The species tree obtained from the BEST analysis recovered a basal trichotomy between a lineage leading to *B. ephippium* and *B. garbeana*, a lineage containing *B. brunneus*, *B. izecksohni*, *B. pombali*, *B. ferruginus*, and *B. pernix*, and another lineage which includes *B. didactylus*, *B. hermogenesi*, *B. alipioi*, *B. pitanga*, *B. vertebralis*, *B. nodoterga*, and *B. toby*. A similar reduction in the resolution of BEST trees has also been observed in other studies (Leaché, 2010; Wiens et al., 2010; Lapoint et al., 2011). Belfiore et al. (2008) remarked that concordance of clade support among individual gene trees results in high support in the BEST approach, whereas discordance among gene trees leads to a reduction in support. This characteristic feature of the interaction between individual gene trees and the BEST approach seems to have determined the outcome of the topology for the BEST tree generated here for *Brachycephalus*.

In spite of the reduced degree of resolution shown by the BEST topology, the analysis of the log likelihoods suggests that the more complex model implemented in BEST explains the multilocus *Brachycephalus* data better than the Bayesian analysis of the concatenated data. The trichotomy shown by the BEST tree might reflect the simultaneous differentiation of the three lineages from a common ancestor. On the other hand, it is quite conceivable that the dataset currently available to us is insufficient for the BEST approach to resolve the branching order of phylogenetic relationships in *Brachycephalus*. Sampling issues such as number of individuals, loci, and sites or the information content of loci are possibly involved in the reduction of node support in trees estimated by the BEST approach (Brito and Edwards, 2009; Knowles, 2009). In any event, the results presented here make it quite clear that the additional sampling of loci, individuals, and populations will be necessary in order to better understand the phylogenetic relationhips of *Brachycephalus*.

### 4.2. Phenotypic diversity

Miniaturization is a phylogenetic reduction in body size (Hanken and Wake, 1993). All species of *Brachycephalus* have a snout–vent length less than 18 mm (Haddad et al., 2010), which is a length smaller than the threshold of 20 mm that defines miniaturization in amphibians (Clarke, 1996; Yeh, 2002). According to this criterion, miniaturization is a unique characteristic of all the species of *Brachycephalus*, and it is not shared with species in the sister genus *Ischnocnema* (Hedges et al., 2008). The process of miniaturization has dramatic effects on amphibian organismal biology, producing reduction in size and structural simplification (Hanken and Wake, 1993), increased morphological variation (Hanken, 1993), hyperossification (Trueb and Alberch, 1985; Yeh, 2002), and novel morphologies (Hanken, 1993). Reduction and structural simplification are well documented in *Brachycephalus* and appear as a loss of phalanges in the manus and pes, a reduced number of functional fingers and toes, and the loss of skull bones, such as the columella, palatine, and quadratojugal (Yeh, 2002; Silva et al., 2007; Frost, 2009; Haddad et al., 2010).

Our geometric-statistical analyses of landmark coordinates revealed marked morphological variation in cranial shape among the species of *Brachycephalus* that is clearly associated with the gradient of mineralization and hyperossification of the skull and post-cranial skeleton. We also demonstrated a significant association between genetic distances estimated from the mtDNA and nuclear loci and variation in cranial shape, measured as Procrustes distances. However, given that the tree generated by the BEST approach did not resolve the basal relationships among the *Brachycephalus* species we cannot at this point infer the evolutionary pattern of origin of the different conditions of mineralization of the skeleton. However, *B. ephippium* and *B. garbeana* which are predicted to be sister-species in the individual and concatenated gene trees and also in the BEST species tree share the hyperossified condition of the skull. Furthermore, these species are uniquely defined by the presence of an evolutionary novelty, the hyperossified dorsal plate (Trueb and Alberch, 1985; Hanken, 1993; Clemente-Carvalho et al., 2009). Evolutionary novelties are defined from a structural standpoint as derived individualized body parts, a definition that highlights the developmental and genetic aspects associated with the origin of novelties (Wagner and Lynch, 2010). From an ontogenetic perspective, the origin of the hyperossified dorsal shield in *B. ephippium* and *B. garbeana* has been recently revealed by electron microscopy of differentially sized specimens (Clemente-Carvalho et al., 2011). Hyperossification begins in juveniles at each end of the fourth and fifth vertebrae and increases laterally and inward as individuals grow, until the hyperossification centers coalesce and generate the adult dorsal shield (Clemente-Carvalho et al., 2011). Thus, from an ontogenetic perspective the origin of the hyperossified dorsal plate in *B. ephippium* and *B. garbeana* is now understood, opening the door for investigations on the genetic-developmental basis of this morphological novelty.

## Acknowledgments

This research was funded by the Conselho Nacional de Desenvolvimento Científico e Tecnológico (CNPq; 470041/2006-4) and Fundação de Amparo à Pesquisa do Estado de São Paulo (FAPESP; 2005/55449-6 and 2008/50928-1). We are indebted to A.S. Abe, A.V.L. Freitas, and M.S. Araújo for reviews, suggestions, and criticisms that helped to improve the manuscript. R.J. Sawaya and T.H. Condez kindly made available some of the samples used in this study. We thank R. Brunetto for image processing. R.B.G. Clemente-Carvalho was supported by a doctoral scholarship from CNPq (141629/2008-8). We are thankful to the two anonymous reviewers whose comments and suggestions went a long way to improve the quality of the manuscript. A.C.R. Alves' work was supported by a postdoctoral FAPESP fellowship (2003/12396-4). The work of S.I. Perez is supported by the Consejo Nacional de Investigaciones Científicas y Técnicas, Argentina. The work of C.F.B. Haddad and S.F. dos Reis is supported by research fellowships from CNPq.

## References


Adams, D.C., Rohlf, F.J., Slice, D.E., 2004. Geometric morphometrics: ten years of progress following the 'revolution'. Ital. J. Zool. 71, 5–16.

Altschul, S.F., Madden, T.L., Schäffer, A.A., Zhang, J., Zhang, Z., Miller, W., Lipman, D.J., 1997. Gapped BLAST and PSI-BLAST: a new generation of protein database search programs. Nucleic Acid Res. 25, 3389–3402.

Alves, A.C.R., Ribeiro, L.F., Haddad, C.F.B., Reis, S.F., 2006. Two new species of *Brachycephalus* (Anura: Brachycephalidae) from the Atlantic forest in Paraná State, southern Brazil. Herpetologica 62, 221–233.

Alves, A.C.R., Sawaya, R., Reis, S.F., Haddad, C.B.F., 2009. A new species of *Brachycephalus* (Anura: Brachycephalidae) from the Atlantic rain forest in São Paulo state, Southeastern Brazil. J. Herp. 43, 212–219.

Ballard, J.W.O., Whitlock, M.C., 2004. The incomplete natural history of mitochondria. Mol. Ecol. 13, 729–744.

Belfiore, N.M., Liu, L., Moritz, C., 2008. Multilocus phylogenetics of a rapid radiation in the genus *Thomomys* (Rodentia: Echimyidae). Syst. Biol. 57, 294–310.

Bookstein, F.L., 1991. Morphometric Tools for Landmark Data. Cambridge University Press, New York.

Brito, P.H., Edwards, S.V., 2009. Multilocus phylogeography and phylogenetics using sequence-based markers. Genetica 135, 439–455.

Castillo-Ramirez, S., Liu, L., Pearl, D., Edwards, S.V., 2010. Bayesian estimation of species trees: a practical guide to optimal sampling and analysis. In: Knowles, L.L., Kubatko, L.S. (Eds.), Estimating Species Trees: Practical and Theoretical Aspects. Wiley-Blackwell, pp. 15–34.

Clarke, B.T., 1996. Small size in amphibians: its ecological and evolutionary implications. Symp. Zool. Soc. Lond. 69, 201–224.

Clemente-Carvalho, R.B.G., Monteiro, L.R., Bonato, V., Rocha, H., Pereira, G., Oliveira, D., Lopes, R., Haddad, C.F.B., Martins, E.G., Reis, S.F., 2008. Geographic variation in cranial shape in the pumpkin toadlet (*Brachycephalus ephippium*): a geometric analysis. J. Herp. 42, 176–185.

Clemente-Carvalho, R.B.G., Antoniazzi, M., Jared, C., Haddad, C.F.B., Alves, A.C.R., Rocha, H.S., Pereira, G.R., Oliveira, D.F., Lopes, R.T., Reis, S.F., 2009. Hyperossification in miniaturized toadlets of the genus *Brachycephalus* (Amphibia: Anura: Brachycephalidae): Microscopic structure and macroscopic patterns of variation. J. Morph. 270, 1285–1295.

Clemente-Carvalho, R.B.G., Alves, A.C.R., Perez, S.I., Haddad, C.F.B., Reis, S.F., 2011. Morphological and molecular variation in the pumpkin toadlet, *Brachycephalus ephippium* (Anura: Brachycephalidae). J. Herp. 45, 194–199.

Cochran, D.M., 1955. Frogs from Southeastern Brazil. US Nat. Mus. Bull. 206, 1–423.

Darst, C.R., Cannatella, D.C., 2004. Novel relationships among hyloid frogs inferred from 12S and 16S mitochondrial DNA sequences. Mol. Phylogenet. Evol. 31, 462–475.

Degnan, J.H., Rosenberg, N.A., 2009. Gene tree discordance, phylogenetic inference and the multispecies coalescent. Trends Ecol. Evol. 24, 332–340.

Dubois, A., 2004. Developmental pathway, speciation and supraspecific taxonomy in amphibians. I. Why are there so many frog species in Sri Lanka? Alytes 22, 19–37.

Edwards, S.V., Liu, L., Pearl, D.K., 2007. High-resolution species trees without concatenation. PNAS 104, 5936–5941.

Ewing, B., Hillier, L., Wendl, M.C., Green, P., 1998. Base-calling of automated sequencer traces using phred. I. Accuracy assessment. Gen. Res. 8, 175–185.

Fabrezi, M., 2006. Morphological evolution of Ceratophryinae (Anura, Neobatrachia). J. Zool. Syst. Evol. Res. 44, 153–166.

Frost, D.R., 2009. Amphibian Species of the World: An Online Reference. Version 3.0. Electronic Database. American Museum of Natural History, New York, New York, USA (22 August 2004). <http://research.amnh.org/herpetology/amphibia/index.html>.

Giaretta, A.A., Sawaya, R.J., 1998. Second species of *Psyllophryne* (Anura: Brachycephalidae). Copeia 1998, 985–987.

Goebel, A.M., Donnelly, J.M., Atz, M.E., 1999. PCR primers and amplification methods for 12S ribosomal DNA, the control region, cytochome oxidase I, and cytochrome *b* in bufonids and other frogs, and an overview of PCR primers which have amplified DNA in amphibians successfully. Mol. Phylogenet. Evol. 11, 163–199.

Gower, J.C., 1971. Statistical methods of comparing different multivariate analyses of the same data. In: Hodson, F.R., Kendall, D.G., Tautu, P. (Eds.), Mathematics in the Archaeological and Historical Sciences. Edinburgh University Press, pp. 138–149.

Haddad, C.F.B., Alves, A.C.R., Clemente-Carvalho, R.B.G., Reis, S.F., 2010. A new species of *Brachycephalus* from the Atlantic Rain Forest in São Paulo State, Southeastern Brazil (Amphibia: Anura: Brachycephalidae). Copeia 2010, 410–420.

Hanifin, C.T., 2010. The chemical and evolutionary ecology of Tetrodotoxin toxicity in terrestrial vertebrates. Mar. Drugs 8, 577–593.

Hanken, J., 1993. Adaptation of bone growth to miniaturization of body size. In: Hall, B.K. (Ed.), Bone Growth. CRC Press, pp. 79–104.

Hanken, J., Wake, D.B., 1993. Miniaturization of body size: organismal consequences and evolutionary significance. Ann. Rev. Ecol. Syst. 24, 501–519.

Hedges, S.B., Duellman, W.E., Heinicke, M.P., 2008. New World direct-development frogs (Anura: Terrarana): molecular phylogeny, classification, biogeography, and conservation. Zootaxa 1737, 1–182.

Heinicke, M.P., Duellman, W.E., Hedges, S.B., 2007. Major Caribbean and Central American frog faunas originated by ancient oceanic dispersal. Proc. Natl. Acad. Sci. (USA) 104, 10092–10097.

Heinicke, M.P., Duellman, W.E., Trueb, L., Means, D.B., MacCulloch, R.D., Hedges, S.B., 2009. A new frog family (Anura: Terrana) from South America and an expanded direct-developed clade revealed by molecular phylogeny. Zootaxa 2211, 1–35.

Huelsenbeck, J.P., Rannala, B., 2004. Frequentist properties of Bayesian posterior probabilities of phylogenetic trees under simple and complex substitution models. Syst. Biol. 53, 904–913.

Huelsenbeck, J.P., Ronquist, F., 2001. MRBAYES: Bayesian inference in phylogeny. Bioinformatics 17, 754–755.

Izecksohn, E., 1971. Novo gênero e nova espécie de Brachycephalidae no estado do Rio de Janeiro. Brasil. Bol. Mus. Nac. Zool. 280, 1–12.

Klingenberg, C.P., Barluenga, M., Meyer, A., 2002. Shape analysis of symmetric structures: quantifying variation among individuals and asymmetry. Evolution 56, 1909–1920.

Knowles, L.L., 2009. Estimating species trees: methods of phylogenetic analysis when there is incongruence across genes. Syst. Biol. 58, 463–467.

Knowles, L.L., Kubatko, L.S., 2010. Estimating species trees: an introduction to concepts and models. In: Knowles, L.L., Kubatko, L.S. (Eds.), Estimating Species Trees: Practical and Theoretical Aspects. Wiley-Blackwell, pp. 1–14.

Lapoint, R.T., Gidaya, A., ÓGrady, P.M., 2011. Phylogenetic relationships in the spoon tarsus subgroup of Hawaiian *drosophila*: conflict and concordance between gene trees. Mol. Phylogenet. Evol. 58, 492–501.

Larkin, M.A., Blackshields, G., Brown, N.P., Chenna, R., McGettigan, P.A., McWilliam, H., Valentin, F., Wallace, I.M., Wilm, A., Lopez, R., Thompson, J.D., Gibson, T.J., Higgins, D.G., 2007. Clustal W and Clustal X version 2.0. Bioinformatics 23, 2947–2948.

Larson, P.M., 2004. Chondrocranial morphology and ontogenetic allometry in larval *Bufo americanus* (Anura, Bufonidae). Zoomorphology 123, 95–106.

Leaché, A.D., 2010. Species trees for spiny lizards (Genus *Sceloporus*): identifying points of concordance and conflict between nuclear and mitochondrial data. Mol. Phylogenet. Evol. 54, 162–171.

Liu, L., 2008. BEST: Bayesian estimation of species trees under the coalescent model. Bioinformatics 24, 2542–2543.

Liu, L., Pearl, D.K., 2007. Species trees from gene trees: reconstructing Bayesian posterior distributions of a species phylogeny using estimated gene tree distributions. Syst. Biol. 56, 504–514.

Liu, L., Yu, L., Kubatko, L., Pearl, D.K., Edwards, S.V., 2009. Coalescent methods for estimating species trees. Mol. Phylogenet. Evol. 53, 320–328.

Lynch, J.D., Duellman, W.E., 1997. Frogs of the genus *Eleutherodactylus* in western Ecuador. U. Kansas Spec. Publ., 23, 1–236.

Mossel, E., Vigoda, E., 2005. Phylogenetic MCMC algorithms are misleading on mixtures of trees. Science 309, 2207–2209.

Pasachnik, S.A., Echternacht, A.C., Fitzpatrick, B.M., 2010. Gene trees, species and species trees in the *Ctenosaura palearis* clade. Conserv. Genet. 11, 1767–1781.

Peres-Neto, P.R., Jackson, D.A., 2001. The importance of scaling of multivariate analyses in ecological studies. Ecoscience 8, 522–526.

Piel, W.H., Chan, L., Dominus, M.J., Ruan, J., Vos, R.A., Tannen, V., 2009. Treebase v.2: A Database of Phylogenetic Knowledge. e-Biosphere.

Pimenta, B.V.S., Bérnils, R.S., Pombal, J.P., 2007. Amphibia, Anura, Brachycephalidae, *Brachycephalus hermogenesi*: filling gap and geographic distribution map. Check List 3, 277–279.

Pires, O.R., Sebben, A., Schwartz, E.F., Largura, S.W.R., Bloch, C., Morales, R.A.V., Schwartz, C.A., 2002. Occurrence of tetradotoxin and its analogues in the Brazilian frog *Brachycephalus ephippium* (Anura: Brachycephalidae). Toxicon 40, 761–766.

Pires, O.R., Sebben, A., Schwartz, E.F., Morales, R.A.V., Bloch, C., Schwartz, C.A., 2005. Further report of the occurrence of tetradotoxin and new analogues in the Anuran family Brachycephalidae. Toxicon 45, 73–79.

Pombal, J.R., 2001. A new species of *Brachycephalus* (Anura: Brachycephalidae) from Atlantic Rain Forest of southeastern Brazil. Amphibia-Reptilia 22, 179–185.

Pombal, J.R., 2010. A posição taxonômica das "variedades" de *Brachycephalus ephippium* (Spix, 1824) descritas por Miranda-Ribeiro, 1920 (Amphibia, Anura, Brachycephalidae). Bol. Mus. Nac. 526, 1–12.

Pombal, J.P., Gasparini, J.L., 2006. A new *Brachycephalus* (Anura: Brachycephalidae) from the Atlantic Rainforest of Espírito Santo, southeastern Brazil. South Am. J. Herp. 1, 87–93.

Pombal, J.P., Wistuba, E.M., Bornschein, M.R., 1998. A new species of Brachycephalid (Anura) from the Atlantic Rain Forest of Brazil. J. Herp. 32, 70–74.

Posada, D., 2008. JModelTest: phylogenetic model averaging. Mol. Biol. Evol. 25, 1253–1256.

R Development Core Team, 2010. R: A Language and Environment for Statistical Computing. R Foundation for Statistical Computing, Vienna, Austria. <http://www.R-project.org>.

Rambaut, A., Drummond, A.J., 2007. Tracer v1.4. <http://beast.bio.ed.ac.uk/Tracer>.

Ribeiro, L.F., Alves, A.C.R., Haddad, C.F.B., Reis, S.F., 2005. Two new species of *Brachycephalus* from Paraná State, southern Brazil (Anura, Brachycephalidae). Bol. Mus. Nac. Zool. 519, 1–18.

Rocha, H.S., Pereira, G.R., Anjos, M.J., Faria, P., Kellermann, G., Perez, C.A., Tirao, G., Mazzaro, I., Giles, C., Lopes, R.T., 2007. Diffraction enhanced imaging and X-ray fluorescence microtomography to analyze biological samples. X-Ray Spec. 36, 247–253.

Rohlf, F.J., 1993. Relative-warp analysis and an example of its application to mosquito wings. In: Marcus, L.F., Bello, E., Garcia-Valdecasas, A. (Eds.), Contributions to Morphometrics. Museo Nacional de Ciencias Naturales, Madrid, pp. 131–159.

Rohlf, F.J., 2006. Tps-DIG, Digitize Landmarks and Outlines, Version 2.05. [Software and Manual]. Department of Ecology and Evolution, State University of New York at Stony Brook, New-York.
Rohlf, F.J., Slice, D., 1990. Extensions of the Procrustes method for the optimal superimposition of landmarks. Syst. Zool. 39, 40–59.
Ronquist, F., Huelsenbeck, J.P., 2003. MRBAYES 3: Bayesian phylogenetic inference under mixed models. Bioinformatics 19, 1572–1574.
Sambrook, J., Fritsch, E.F., Maniatis, T., 1989. Molecular Cloning: A Laboratory Manual, second ed. Cold Spring Harbor Laboratory Press, New York.
Silva, H.R., Campos, L.A., Sebben, A., 2007. The auditory region of *Brachycephalus* and its bearing on the monophyly of the genus (Anura: Brachycephalidae). Zootaxa 1422, 59–68.
Trueb, L., Alberch, P., 1985. Miniaturization in the anuran skull: a case study of heterochrony. In: Duncker, H.R., Fleischer, G. (Eds.), Vertebrate Morphology. Gustav Fisher Verlag, pp. 113–121.
Verdade, V.K., Rodrigues, M.T., Cassimiro, J., Pavan, D., Liou, N., Lange, M.C., 2008. Advertisement call, vocal activity, and geographic distribution of *Brachycephalus hermogenesi* (Giaretta and Sawaya, 1998) (Anura, Brachycephalidae). J. Herp. 42, 542–549.
Wagner, G.P., Lynch, V.J., 2010. Evolutionary novelties. Curr. Biol. 20, R48–R52.
Wiens, J.J., Kuczynski, C.A., Arif, S., Reeder, T.W., 2010. Phylogenetic relationships of phrynosomatid lizards based on nuclear and mitochondrial data, and a revised phylogeny for *Sceloporus*. Mol. Phylogenet. Evol. 54, 150–161.
Yeh, J., 2002. The effect of miniaturized body size on skeletal morphology in frogs. Evolution 56, 628–641.
Zinc, R.M., Barrowclough, G.F., 2008. Mitochondrial DNA under siege in avian phylogenetics. Mol. Ecol. 17, 2107–2121.